

SIMULATION OF CURVILINEAR MOTION OF AUTOMOBILE WITH THE USE OF TWO-DEGREE-OF-FREEDOM FLAT MODEL

HUBERT SAR¹, MATEUSZ BRUKALSKI², KRZYSZTOF ROKICKI³

Abstract

Development of active safety systems of automobiles is nowadays based not only on road tests, but also on computer simulation of vehicle's curvilinear motion. To properly perform simulation, all required model parameters have to be properly estimated. The less complicated model is, the less parameters it requires. So that, it makes no sense to apply too complicated models, if we are not able to estimate parameters with relatively low error. One of the most popular is two-degree-of-freedom flat model to describe curvilinear motion of automobile. It is widely used in design and improvement of active safety systems.

The article discusses the application of simple two-degree-of-freedom flat model of automobile, which requires only several parameters. These parameters are: mass of a vehicle, location of center of gravity of a vehicle, yaw mass moment of inertia of a vehicle, side-slip characteristics. Furthermore, to be able to compare simulation and measurement results, it is necessary to know some input signals such as steering wheel angle and velocity of a vehicle, recorded during road tests. In this article signal of steering wheel angle was taken from Controller Area Network (CAN) bus.

In case of model of a vehicle, the Authors decided to compare the results of simulation using two different side slip characteristics known as the dependence between lateral reaction force and side slip angle: linear characteristic (constant cornering stiffness) and the characteristic represented by Pacejka's Magic Formula in steady-state version.

Keywords: vehicles; safety; traffic accidents reconstruction; road tests; Magic Formula

1. Introduction

Vehicle's motion modelling is one of the most popular methods of investigating automobiles, including development of their active safety systems. There is, of course, computer software (for example ADAMS,) that is able to simulate vehicle motion. There are also

¹ Institute of Vehicles, Warsaw University of Technology, 84 Narbutta St., 02-524 Warsaw, Polska, e-mail: hubert.sar@pw.edu.pl

² Institute of Vehicles, Warsaw University of Technology, 84 Narbutta St., 02-524 Warsaw, Polska, e-mail: mateusz.brukalski@pw.edu.pl

³ Institute of Vehicles, Warsaw University of Technology, 84 Narbutta St., 02-524 Warsaw, Polska, e-mail: krzysztof.rokicki@pw.edu.pl

specialized computer tools for traffic incidents' reconstruction like PC-Crash or Cyborg Idea V-sim. Very often they use in-built models of a vehicle, models or characteristics of tyres, which cannot be modified. Usually only models' coefficients can be changed.

Another, perhaps better, approach to vehicle motion modelling is to prepare a model of a vehicle from the basics, for particular aim of conducted research. It allows to define the quantity of degrees of freedom adequately for the needs of a research. It is important, because if we have limited number of parameters of a model, often better solution will be the choice of less complicated model, including model of a tyre, for which we are able to estimate certain parameters with acceptable level of error. One of tyres' models can be found in [10], where interaction between pavement and heavy vehicle's tyres takes place, including unevenness of the road. In paper [4] there was shown the application of tyre's model in a form of flexible ring, together with experiments with the use of special test rig for tyres. Next article [15] shows the application of Kelvin-Voigt model in the description of tyre's deformation by applying axial stiffness and damping stiffness. Work [3] shows the example of applying finite element analysis including hyper-elastic rubber properties. Vertical, longitudinal and lateral tyre's stiffness validation tests were performed in [3]. Next paper [18] discusses the tyre's three-dimensional ring model. In work [17] there are compared two physical models of tyres, which are available on the market, together with experimental validation on special test rig. In article [16] there is presented a method of tyres' modelling including low and high tyre-to-road adhesion coefficient, together with the application in vehicle's motion model.

Another not less important issue is proper description of side slip phenomenon. It can be achieved through side slip characteristics or by more complicated models of tyres. In paper [2] there are presented side slip angles observers, together with two-track flat model of automobile as extended version of very popular the so-called "bicycle model". However, application of signals, which help obtain side slip angles, but are not directly connected with wheels, requires proper filtration, for example Kalman's filtering. Next article [9] shows the method of obtaining side slip angles through image processing. Work [5] contains vehicle's side slip estimation using information from CAN-C, again applying Kalman's filtration procedure. In [8] single track "bicycle" model is used together with exponential equation describing dependence between transverse reaction pavement-to-tyre force and side slip angle. Example of a model of a vehicle with many degrees of freedom and many parameters describing its systems is truck model presented by Lozia [11]. Interaction inside the system driver-vehicle-road environment is shown by [14]. Simulation of vehicle's motion becomes more complex, if we discuss both lateral and radial vibrations, which is discussed in [18]. Discussing tyre models, there can be found many approaches to tyres' modelling. One of them is Pacejka's semi empirical model with well-known Magic Formula [13]. As presented in [1], this model is very popular in the development of active safety systems. Another issue is the application of the models available on the market in multibody-simulation as presented in [17]. These models presented in [17] are applied, as they used to be optimal for driving comfort and vertical vibrations analysis. Another the so-called brush model was presented mentioned by [1], as proper for vehicle dynamics and driving stability. Another approach to tyres' modelling is the application of finite element method (FEM) as depicted in [12].

2. Presentation of model applied for the research

Model applied in this work simplified version of the model shown in Figure 1. It means that vehicle's longitudinal velocity was assumed as constant and vehicle's body roll and pitch motion were skipped.

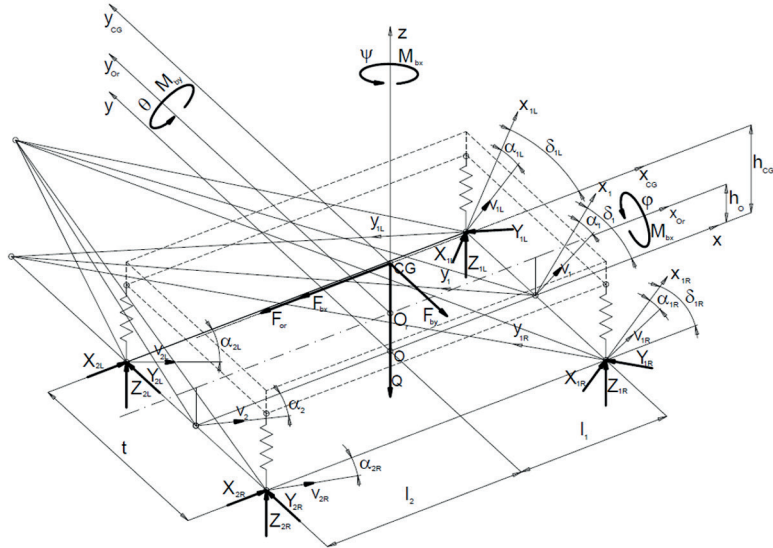


Fig. 1. Scheme of a vehicle's model

In Table 1 there are presented data applied for investigation of the vehicle Hyundai Veloster. Steering system ratio depicted in Table 1 was assumed as average for the whole range of steering wheel angle. Ackermann's dependence was skipped in this article. Both suspension and tyre vertical stiffnesses were not included.

Tab. 1. Basic parameters applied during simulation

Vehicle's mass m [kg]	1419
Wheelbase l_{12} [m]	2.650
Distance between front axle and vehicle's center of mass l_1 [m]	1.089
Vehicle's yaw mass moment of inertia I_z [kgm ²]	2100
Average wheel track t [m]	1.560
Average steering system ratio i_k [-]	15.1
Tyre-to-road adhesion coefficient μ [-]	0.90

Equations of vehicle's motion are presented below.

$$F_{bx} = X_{1R} \cdot \cos\delta_{1R} + X_{2R} + X_{1L} \cdot \cos\delta_{1L} + X_{2L} - Y_{1R} \cdot \sin\delta_{1R} - Y_{1L} \cdot \sin\delta_{1L} - F_{Or} \quad (1)$$

$$m \cdot \ddot{x} = X_{1R} \cdot \cos\delta_{1R} + X_{2R} + X_{1L} \cdot \cos\delta_{1L} + X_{2L} - Y_{1R} \cdot \sin\delta_{1R} - Y_{1L} \cdot \sin\delta_{1L} - F_{Or} \quad (2)$$

$$F_{by} = X_{1R} \cdot \sin\delta_{1R} + X_{1L} \cdot \sin\delta_{1L} + Y_{1R} \cdot \cos\delta_{1R} + Y_{1L} \cdot \cos\delta_{1L} + Y_{2R} + Y_{2L} \quad (3)$$

$$m \cdot \dot{x} \cdot \dot{\psi} + m \cdot \ddot{y} = X_{1R} \cdot \sin\delta_{1R} + X_{1L} \cdot \sin\delta_{1L} + Y_{1R} \cdot \cos\delta_{1R} + Y_{1L} \cdot \cos\delta_{1L} + Y_{2R} + Y_{2L} \quad (4)$$

$$Q = Z_{1R} + Z_{1L} + Z_{2R} + Z_{2L} \quad (5)$$

$$M_{bx} = (X_{1R} \cdot \sin\delta_{1R} + Y_{1R} \cdot \cos\delta_{1R} + X_{1L} \cdot \sin\delta_{1L} + Y_{1L} \cdot \cos\delta_{1L} + Y_{2R} + Y_{2L}) \cdot h_{CG} + Z_{1L} \cdot \frac{t}{2} - Z_{1R} \cdot \frac{t}{2} + Z_{2L} \cdot \frac{t}{2} - Z_{2R} \cdot \frac{t}{2} \quad (6)$$

$$\begin{aligned} F_{by} \cdot (h_{CG} - h_O) = \\ = (X_{1R} \cdot \sin\delta_{1R} + Y_{1R} \cdot \cos\delta_{1R} + X_{1L} \cdot \sin\delta_{1L} + Y_{1L} \cdot \cos\delta_{1L} + Y_{2R} + Y_{2L}) \\ \cdot h_{CG} + Z_{1L} \cdot \frac{t}{2} - Z_{1R} \cdot \frac{t}{2} + Z_{2L} \cdot \frac{t}{2} - Z_{2R} \cdot \frac{t}{2} \end{aligned} \quad (7)$$

$$(m \cdot \dot{x} \cdot \dot{\psi} + m \cdot \ddot{y}) \cdot (h_{CG} - h_O) = (X_{1R} \cdot \sin\delta_{1R} + Y_{1R} \cdot \cos\delta_{1R} + X_{1L} \cdot \sin\delta_{1L} + Y_{1L} \cdot \cos\delta_{1L} + Y_{2R} + Y_{2L}) \cdot h_{CG} + Z_{1L} \cdot \frac{t}{2} - Z_{1R} \cdot \frac{t}{2} + Z_{2L} \cdot \frac{t}{2} - Z_{2R} \cdot \frac{t}{2} \quad (8)$$

or

$$\begin{aligned} I_x \cdot \ddot{\varphi} = (X_{1R} \cdot \sin\delta_{1R} + Y_{1R} \cdot \cos\delta_{1R} + X_{1L} \cdot \sin\delta_{1L} + Y_{1L} \cdot \cos\delta_{1L} + Y_{2R} + Y_{2L}) \cdot h_{CG} + Z_{1L} \cdot \frac{t}{2} - Z_{1R} \cdot \frac{t}{2} + Z_{2L} \\ \cdot \frac{t}{2} - Z_{2R} \cdot \frac{t}{2} \end{aligned} \quad (9)$$

$$\begin{aligned} M_{by} = (-X_{1R} \cdot \cos\delta_{1R} + Y_{1R} \cdot \sin\delta_{1R} - X_{1L} \cdot \cos\delta_{1L} + Y_{1L} \cdot \sin\delta_{1L} - X_{2R} - X_{2L}) \cdot h_{CG} - Z_{1L} \\ \cdot l_1 - Z_{1R} \cdot l_1 + Z_{2L} \cdot l_2 - Z_{2R} \cdot l_2 \end{aligned} \quad (10)$$

$$\begin{aligned} (F_{Bx} + F_{Or}) \cdot (h_{CG} - h_O) = \\ = (-X_{1R} \cdot \cos\delta_{1R} + Y_{1R} \cdot \sin\delta_{1R} - X_{1L} \cdot \cos\delta_{1L} + Y_{1L} \cdot \sin\delta_{1L} - X_{2R} - X_{2L}) \cdot h_{CG} - Z_{1L} \cdot l_1 \\ - Z_{1R} \cdot l_1 + Z_{2L} \cdot l_2 - Z_{2R} \cdot l_2 \end{aligned} \quad (11)$$

$$\begin{aligned} I_y \cdot \ddot{\theta} = (-X_{1R} \cdot \cos\delta_{1R} + Y_{1R} \cdot \sin\delta_{1R} - X_{1L} \cdot \cos\delta_{1L} + Y_{1L} \cdot \sin\delta_{1L} - X_{2R} - X_{2L}) \cdot h_{CG} - Z_{1L} \cdot l_1 - Z_{1R} \cdot l_1 \\ + Z_{2L} \cdot l_2 - Z_{2R} \cdot l_2 \end{aligned} \quad (12)$$

$$M_{bz} = X_{1L} \cdot \cos\delta_{1L} \cdot \frac{t}{2} - X_{1L} \cdot \sin\delta_{1L} \cdot l_1 - Y_{1L} \cdot \cos\delta_{1L} \cdot l_1 - Y_{1L} \cdot \sin\delta_{1L} \cdot \frac{t}{2} - X_{1R} \cdot \cos\delta_{1R} \cdot \frac{t}{2} - X_{1R} \cdot \sin\delta_{1R} \cdot l_1 - Y_{1R} \cdot \cos\delta_{1R} \cdot l_1 + Y_{1R} \cdot \sin\delta_{1R} \cdot \frac{t}{2} + X_{2L} \cdot \frac{t}{2} + Y_{2L} \cdot l_2 - X_{2R} \cdot \frac{t}{2} + Y_{2R} \cdot l_2 \quad (13)$$

$$I_Z \cdot \ddot{\psi} = X_{1L} \cdot \cos\delta_{1L} \cdot \frac{t}{2} - X_{1L} \cdot \sin\delta_{1L} \cdot l_1 - Y_{1L} \cdot \cos\delta_{1L} \cdot l_1 - Y_{1L} \cdot \sin\delta_{1L} \cdot \frac{t}{2} - X_{1R} \cdot \cos\delta_{1R} \cdot \frac{t}{2} - X_{1R} \cdot \sin\delta_{1R} \cdot l_1 - Y_{1R} \cdot \cos\delta_{1R} \cdot l_1 + Y_{1R} \cdot \sin\delta_{1R} \cdot \frac{t}{2} + X_{2L} \cdot \frac{t}{2} + Y_{2L} \cdot l_2 - X_{2R} \cdot \frac{t}{2} + Y_{2R} \cdot l_2 \quad (14)$$

For the needs of this article some simplifications of the model were made. Longitudinal velocity was assumed as constant. For simulations, as input parameter averaged longitudinal velocity was applied. So, longitudinal inertial forces were skipped. This was justified, because the longitudinal accelerations did not exceed (0.4-0.6) m/s² during the maneuver. During the tests a driver was responsible for keeping the speed constant. The simplifications are shown below:

$$\begin{aligned} \dot{x} &= 0 \\ h_{CG} &= 0 \\ h_0 &= 0 \\ \varphi &= 0 \\ \theta &= 0 \end{aligned}$$

So, taking into account the above mentioned assumptions, the system of differential equations describing vehicle's motion contains equations (4) and (14). After simplifications, the system of differential equations (4) and (14) was solved, representing two-degree-of-freedom model.

To describe the cornering properties of front and rear axle, the dependence between transverse forces and side slip angles of left and right side of axles was applied. It was implemented in two ways. Firstly, it was the most simplified linear dependence between lateral force Y and side slip angle α , using cornering stiffnesses K of left and right sides of front and rear axle. Second approach was the application of Magic Formula in steady-state version, where the linear fragment of Magic Formula coincided with the linear function associated with cornering stiffness.

$$Y = K \cdot \alpha \quad (15)$$

Secondly, there was applied Magic Formula [13] to present the dependence between tangent reaction force Y and side slip angle α . Force Y is also calculated in dependence with normal road - wheel reaction force Z and tyre-to-road adhesion coefficient μ .

$$Y = -\mu \cdot Z \cdot \sin\left(C \cdot \arctg\left(B \cdot \alpha - E \cdot (B \cdot \alpha - \arctg(B \cdot \alpha))\right)\right) \quad (16)$$

In Table 2 there are presented coefficients applied in case of formulas (15) and (16) for front and rear axle.

Tab. 2. Coefficients for equations (17) and (18) applied during simulation

	left, right part of front axle	left, right part of rear axle
cornering stiffness K [N/rad]	80000	105000
<i>B</i>	17	30
<i>C</i>	1.1	1.1
<i>D</i>	$\mu \cdot Z$	$\mu \cdot Z$
<i>E</i>	-15	-15

Figures 2 and 3 show side slip characteristics for front and rear axle. Each characteristic represents respectively left and right side of front (Figure 2) and rear axle (Figure 3).

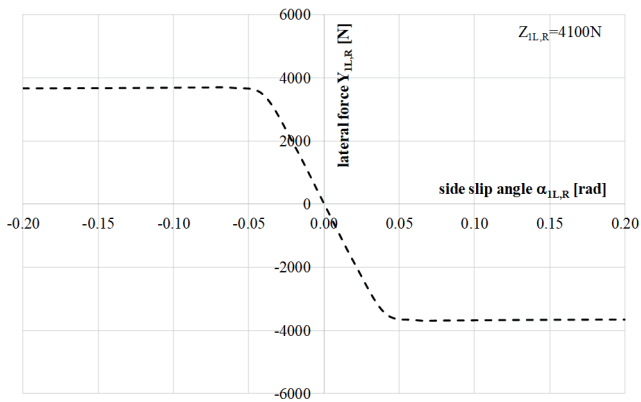


Fig. 2. Side slip characteristic of left or right side of front axle

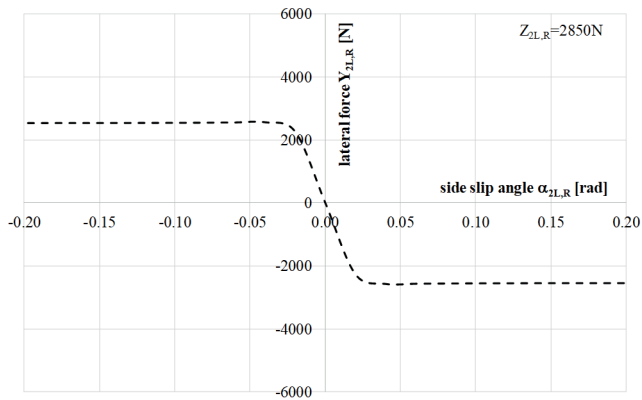


Fig. 3. Side slip characteristic of left or right side of rear axle

The Authors decided to apply for the research the signals from CAN bus, through special measurement card and own software made in LabView environment. Thanks to this approach, it was not necessary to use external sensors of such signals as steering wheel angle, yaw velocity and lateral acceleration. Of course, in the future it is planned to compare CAN bus signals with those measured applying external sensors. Additionally, simple 10 Hz GPS receiver was used to know speed of researched automobile.

Simplified structure of simulation program is presented in Figure 4. Matlab/Simulink environment allowed for solving the system of differential equations (4) and (14).

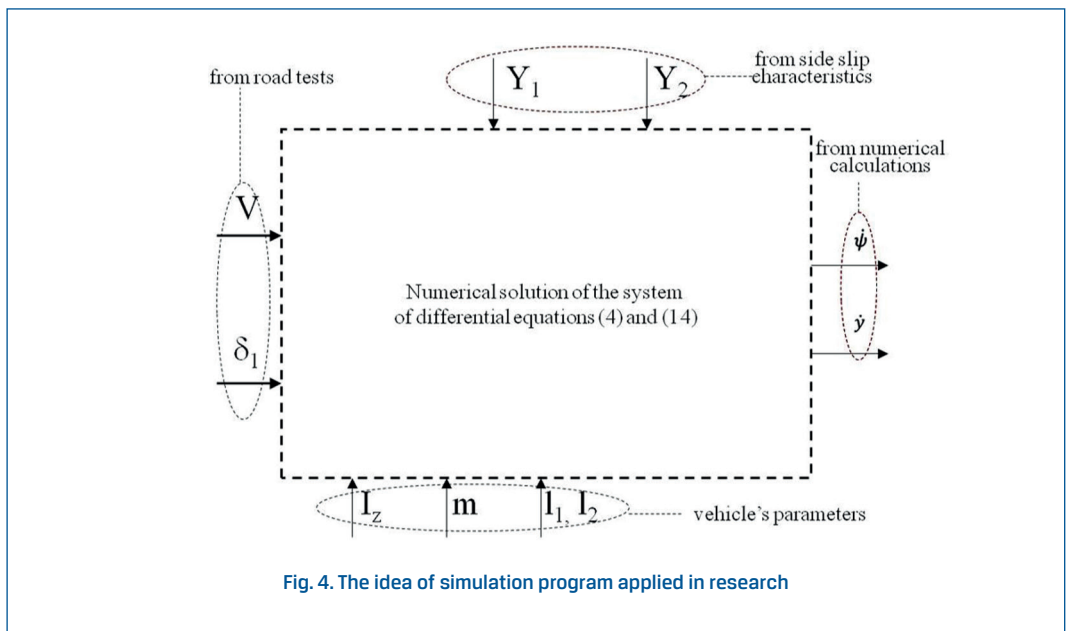


Fig. 4. The idea of simulation program applied in research

3. Exemplary simulation results of vehicle's curvilinear motion

To ensure comparability of road tests with simulation results, the input parameter of the model in a form of steering wheel angle signal was assumed. Also, the information of vehicle's speed came from GPS receiver. During the tests the vehicle's speed was approximately constant. So, for simulations the speed was averaged for each of the tests.

Figure 5 shows front driven Hyundai Veloster applied for road tests.



Fig. 5. Hyundai Veloster during double lane change maneuver

In this chapter there are presented exemplary simulation results of curvilinear motion simulations. They are represented by vehicle's angular, lateral velocity and lateral acceleration in the center of gravity (COG). The Authors presented road tests and simulation results on the basis of two types of maneuvers - double lane change [6] and obstacle avoidance [7].

First type of applied maneuver is described in Figure 6.

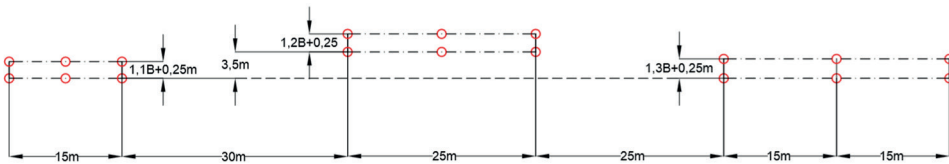


Fig. 6. Scheme of double lane change maneuver according to [6] ISO 3888-1:2018

In Figure 7 we can see the yaw velocity and steering wheel angle courses, including road tests and simulation results for two different side slip characteristics.

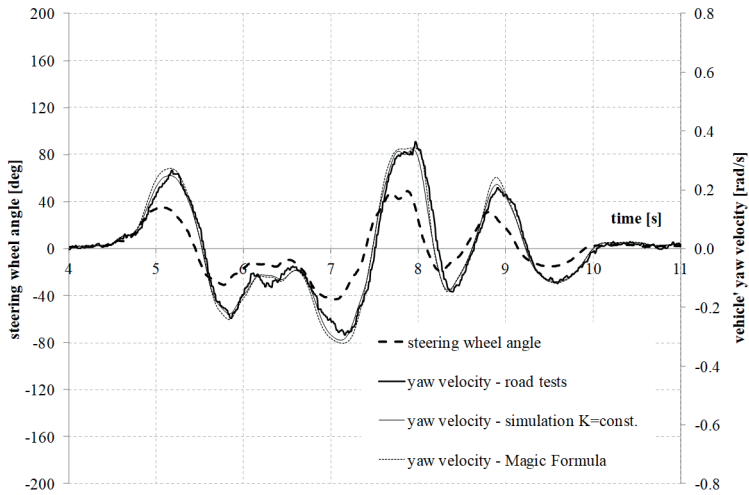


Fig. 7. Vehicle's yaw velocity and steering wheel angle (double lane change test [6] - road test and simulations)

In Figures 8 and 9 there are also depicted respectively the plots of vehicle's lateral velocity and acceleration from road measurements and simulations.

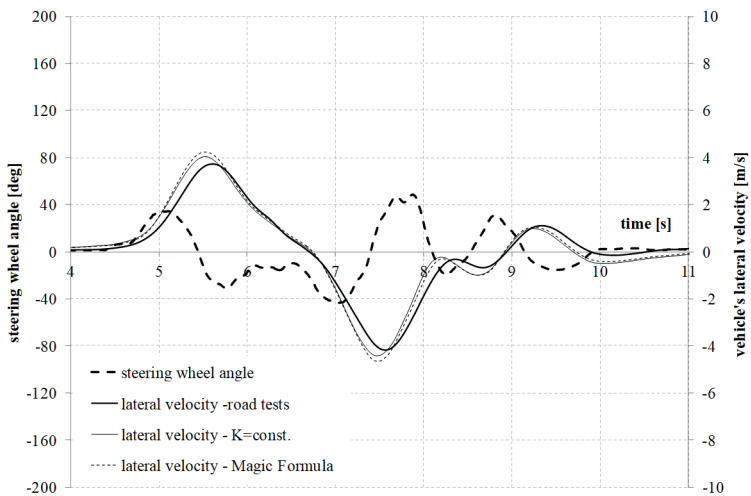


Fig. 8. Vehicle's COG lateral velocity and steering wheel angle (double lane change test [6] - road test and simulations)

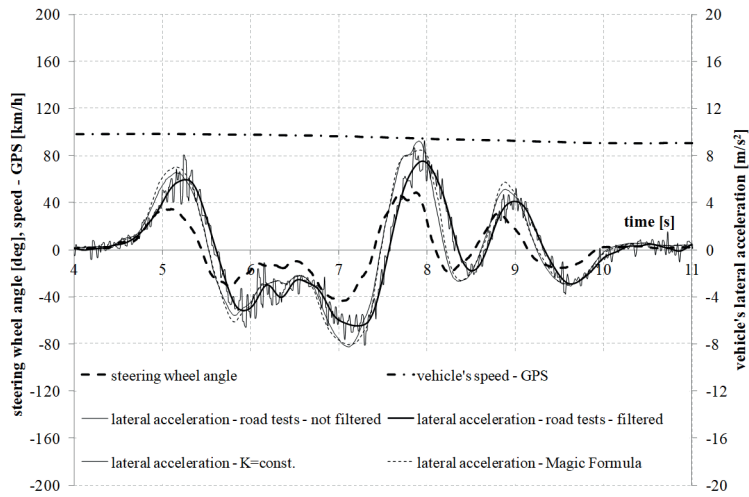


Fig. 9. Vehicle's COG lateral acceleration and steering wheel angle (double lane change test [6] – road test and simulations)

Second type of double lane change attempt is presented in Figure 10.

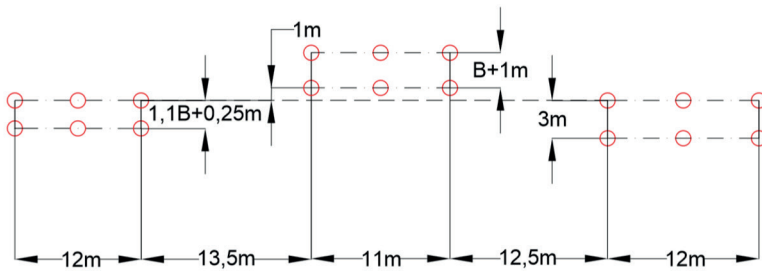


Fig. 10. Scheme of obstacle avoidance maneuver according to ISO 3888-2:2011 [7]

Similar to the previous road test [6], in Figures 11, 12 and 13 there are presented the courses of steering wheel angle, the vehicle's yaw and lateral velocity, and lateral acceleration.

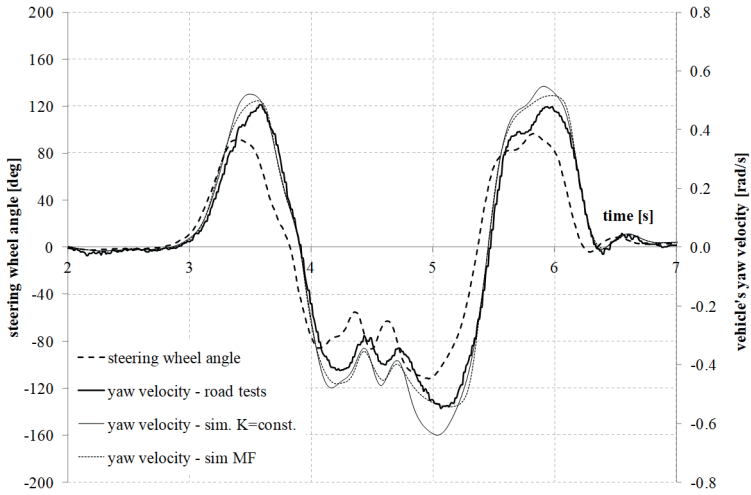


Fig. 11. Vehicle's yaw velocity and steering wheel angle (obstacle avoidance test [7] - road test and simulations)

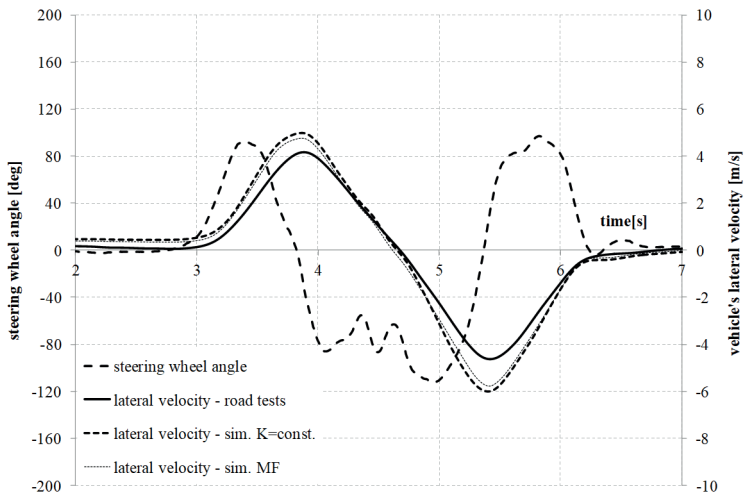


Fig. 12. Vehicle's COG lateral velocity and steering wheel angle (obstacle avoidance test [7] - road test and simulations)

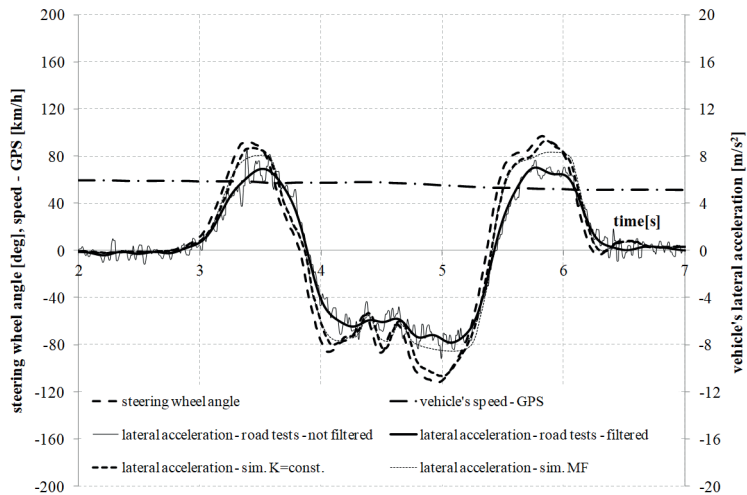


Fig. 13. Vehicle's COG lateral acceleration and steering wheel angle (obstacle avoidance test [7] – road test and simulations)

Maneuver described by ISO 3888-2:2011 is characterized by much shorter length. This is why in case of this test and nearly two times lower vehicle's speed the values of lateral accelerations are comparable.

Simulations were performed for two types of side slip characteristics - linear and non-linear - described by Pacejka's Magic Formula [13]. Special role of non-linear characteristics can be seen on the results of simulation of ISO 3888-2:2011. This is because of higher side slip angles in this maneuver (about two times higher are the peak values of steering wheel angle). Linear side slip characteristics are not enough in this maneuver's simulation, because for higher values of side slip angles they do not limit the lateral forces, not recognizing full lateral slip. For maneuvers with higher level of lateral dynamics it is necessary to include the saturation of road-tyre lateral forces, which represents full side slip. In [14] it is suggested to apply linear dependence between lateral forces and side slip angles until lateral acceleration exceeds 0.4 g.

4. Conclusion

It is worth continuing works on the development of vehicle's motion modelling, especially curvilinear motion. It requires proper mathematical model of a vehicle. What is more problematic, some input signals are usually needed. In case of this article it was steering wheel angle and vehicle's speed which was practically constant during performed tests, and taken from GPS receiver. The original feature of the article is that the model's input parameter (steering wheel angle) came from CAN-C network of the vehicle. The yaw velocity signal and lateral acceleration signal also came from CAN-C, to which the ESP control unit

is assigned. So that, there should be no time shift between analyzed signals. However, this fact should be confirmed in future works, applying inertial measurement unit (IMU) or GPS system based on reference stations. Presented results look promising and, for example, to be able to deeper analyze the on-board signals, special filtration procedure should be developed, for example Kalman's filtration. This would allow to observe side slip angles of front and rear axle. Despite the fact, that two-degree-of-freedom model is quite popular in the development of active safety systems, in the future the Authors are planning to unlock the roll and pitch motion in vehicle's model. More complex motion of the vehicle (braking or accelerating together with cornering) will be modelled. It will be, in particular, the adjustment of the distribution of tractive forces on drive axle and its influence on the vehicle's steerability. To achieve this, side slip angles of front and rear axle will be estimated with the use of yaw velocity and integrated lateral acceleration. Also Pacejka's non-steady-state Magic Formula will be implemented, together with identification of its parameters, using Monte Carlo, genetic algorithm or neural network method.

5. Nomenclature

$1, 2$ – front, rear axle

L, R – left right side of the axles

I_X, I_Y, I_Z – mass moments of inertia (respectively roll, pitch and yaw)

φ – vehicle body's roll angle

θ – vehicle body's pitch angle

ψ – vehicle body's yaw angle

δ – wheel's steering angle

X, Y, Z – pavement-to-tyre reaction force (longitudinal, lateral, vertical)

F_{or} – resultant drag force

Q – weight of a vehicle

M_{bx}, M_{by}, M_{bz} – torque of inertia resistance (longitudinal, lateral, vertical)

h_{CG} – height of the center of gravity (COG)

h_O – height of vehicle's roll axis

\dot{x}, \ddot{x} – respectively longitudinal velocity, acceleration

\dot{y}, \ddot{y} – respectively lateral COG velocity, acceleration

$v_{1L}, v_{1R}, v_{2L}, v_{2R}$ – resultant velocities of wheels

α – side slip angle

i_k – average steering system ratio

t – wheels' track

μ – tyre-to-road adhesion coefficient

B, C, D, E – coefficients in Magic Formula

K – cornering stiffness

References

- [1] Ammon D.: Vehicle dynamics analysis tasks and related tyre simulation challenges. *Vehicle System Dynamics*. 2005, 43(Sup. 1), 30–47, DOI: 10.1080/00423110500141003.
- [2] Cheng S., Li L., Yan B., Liu C., Wang X., Fang J.: Simultaneous estimation of tire side-slip angle and lateral tire force for vehicle lateral stability control. *Mechanical Systems and Signal Processing*. 2019, 132, 168–182, DOI: 10.1016/j.ymssp.2019.06.022.
- [3] El-Sayegh Z., Sharifi M., Gheshlaghi F., Mardani A.: Development of an HLFS agricultural tire model using FEA technique. *SN Applied Sciences*. 2019, 1454(1), DOI: 10.1007/s42452-019-1524-y.
- [4] Garcia-Pozuelo D., Olatunbosun O. A., Romano L., Strano S., Terzo M., Tuononen A.J. et al.: Development and experimental validation of a real-time analytical model for different intelligent tyre concepts. *Vehicle System Dynamics*. 2019, 57(12), 1970–1988, DOI: 10.1080/00423114.2019.1566560.
- [5] Hyun M., Cho W.: Estimation of Road Bank Angle and Vehicle Side Slip Angle Using Bayesian Tracking and Kalman Filter Approach. *International Journal of Automotive Technology*. 2018, 19(6), 993–1000, DOI: 10.1007/s12239-018-0096-y.
- [6] ISO 3888-1:2018, Passenger cars - Test track for a severe lane-change manoeuvre - Part 1: Double lane-change.
- [7] ISO 3888-2:2011, Passenger cars - Test track for a severe lane-change manoeuvre - Part 2: Obstacle avoidance.
- [8] Jin C., Shao L., Lex C., Eichberger A.: Vehicle Side Slip Angle Observation with Road Friction Adaptation. *IFAC-PapersOnLine*. 2017, 50(1), 3406–3411, DOI: 10.1016/j.ifacol.2017.08.593.
- [9] Johnson DK., Botha TR., Els PS.: Real-time side-slip angle measurements using digital image correlation. *Journal of Terramechanics*. 2019, 81, 35–42, DOI: 10.1016/j.jterra.2018.08.001.
- [10] Kansake B. A., Frimpong S.: Analytical modelling of dump truck tire dynamic response to haul road surface excitations. *International Journal of Mining, Reclamation and Environment*. 2020, 34(1), 1–18, DOI: 10.1080/17480930.2018.1507608.
- [11] Lozia Z.: Rollover Thresholds of the Biaxial Truck During Motion on an Even Road. *Vehicle System Dynamics*. 1998, 29(Sup. 1), 735–740, DOI: 10.1080/00423119808969601.
- [12] Nakashima H., Wong JY.: A three-dimensional tire model by the finite element method. *Journal of Terramechanics*. 1993, 30(1), 21–34, DOI: 10.1016/0022-4898(93)90028-V.
- [13] Pacejka HB.: *Tire and Vehicle Dynamics*. Elsevier, 2012.
- [14] Reński A.: Analysis of the Influence of the Drive Force Distribution Between Axles on an Automobile Stability in Its Curvilinear Motion. Springer International Publishing Switzerland 2017 A. Chiru and N. Ispas (eds.), CONAT 2016 International Congress of Automotive and Transport Engineering. DOI 10.1007/978-3-319-45447-4_6.
- [15] Sandu C., Taheri S., Taheri S., Gorsich D.: Hybrid Soft Soil Tire Model (HSSTM). Part I: Tire material and structure modeling. *Journal of Terramechanics*. 2019, 86, 1–13, DOI:10.1016/j.jterra.2019.08.002.
- [16] Sun X., Zhang H., Cai Y., Wang S., Chen L.: Hybrid modeling and predictive control of intelligent vehicle longitudinal velocity considering nonlinear tire dynamics. *Nonlinear Dynamics*. 2019, 97, 1051–1066, DOI: 10.1007/s11071-019-05030-5.
- [17] Uhlar S., Heyder F., König T.: Assessment of two physical tyre models in relation to their NVH performance up to 300 Hz. *Vehicle System Dynamics*. 2019, 1–21, DOI: 10.1080/00423114.2019.1681475.
- [18] Yu X., Huang H., Zhang T.: A theoretical three-dimensional ring based model for tire high-order bending vibration. *Journal of Sound and Vibration*. 2019, 459, 114820, DOI: 10.1016/j.jsv.2019.06.027.